

Random matrix model for chiral symmetry breaking

A. D. Jackson and J. J. M. Verbaarschot

Department of Physics, SUNY, Stony Brook, New York 11794

(Received 25 September 1995)

We formulate a random matrix model which mimics the chiral phase transition in QCD with two light flavors. Two critical exponents are calculated. We obtain the mean-field values $\beta=1/2$ and $\delta=3$. We also find that the chiral phase transition can be characterized by the dynamics of the smallest eigenvalue of the Dirac operator. This suggests an alternative order parameter which may be of relevance for lattice QCD simulations. [S0556-2821(96)05710-4]

PACS number(s): 12.38.Aw, 11.30.Qc, 11.30.Rd, 24.60.Ky

I. INTRODUCTION

In recent years, the QCD phase transition has been studied in a variety of ways using both numerical simulations and analytical methods. Such studies have led to the conviction that it may be a second-order phase transition [1,2]. As has been stressed, in particular in [3,4], this has important consequences because the transition can then be characterized by critical exponents corresponding to a specific universality class. In particular, it was argued that the critical exponents are those of an O(4) Heisenberg spin model. [On a lattice and with Kogut-Susskind fermions, the relevant model might rather be an O(2) spin model.] However, as always, universality arguments must be used with care. According to a recent suggestion in [5] based on simulations of the three-dimensional Gross-Neveu model, they may not be valid for phase transitions involving soft modes composed of fermions. The reason is that the lowest Matsubara frequency suppresses infrared divergences which lead to the universal critical exponents. Indeed, Kocic and Kogut found that the critical exponents in their model are given by mean-field theory.

We wish to study the chiral phase transition from the perspective of the spectrum of the Euclidean Dirac operator. Although initial numerical lattice results regarding this issue have become available [6,7,2], systematic study is beyond the reach of present day computers. Thus, we prefer to construct a simple model which not only contains the global symmetries of QCD but also reproduces mean-field critical exponents. The zero-temperature version of this model was considered previously [8], and it was shown [9] that it is equivalent to the finite-volume effective partition function. In particular, it was shown [8] that the spectrum of the Dirac operator in this random matrix model obeys the so-called Leutwyler-Smilga sum rules [10].

In this work we consider the nonzero-temperature results of two versions of the random matrix model, for SU(2) and for SU(N_c), $N_c \geq 3$ both with fundamental fermions, which are characterized by real and complex matrix elements, respectively. In agreement with [5], temperature dependence is introduced by complementing the zero-temperature random matrix model with the temperature dependence of the lowest Matsubara frequency (see Sec. II). In Sec. III we show that this temperature dependence indeed leads to mean-field critical exponents. Contrary to QCD, our model shows a second-

order phase transition independent of the number of flavors. Therefore, it only models QCD with two light flavors. However, because of the weak flavor dependence of our model, we expect that the quenched approximation is better than for QCD. For this reason and because unquenched simulations are very expensive even for this simple model the Dirac spectrum and the chiral condensate are studied numerically in Secs. IV and V by using the quenched approximation ($N_f=0$). In Sec. IV the temperature dependence of the spectrum and the dependence of the chiral condensate on the valence quark mass are calculated. The latter quantity is found to be in qualitative agreement with recent lattice calculations [2]. The dynamics of the smallest eigenvalue are studied in Sec. V.

II. FINITE-TEMPERATURE CHIRAL RANDOM MATRIX MODEL

The QCD partition function for vacuum angle θ is defined as

$$Z_{\text{QCD}} = \sum_{\nu} e^{i\nu\theta} Z_{\text{QCD}}(\nu), \quad (2.1)$$

where the partition function in a sector with topological charge ν and N_f fermionic flavors is given by

$$Z_{\text{QCD}}(\nu) = \left\langle \prod_{f=1}^{N_f} m_f^{\nu} \prod_{\lambda_n > 0} (\lambda_n^2 + m_f^2) \right\rangle_A. \quad (2.2)$$

Here, $(\dots)_A$ denotes the average over all gauge field configurations, with topological charge ν weighted according to the QCD action. The eigenvalues, λ_{κ} , of the Dirac operator fluctuate over the ensemble of gauge field configurations. In general, the complete eigenvalue density is determined in a non-trivial way by the dynamics of QCD. However, the fluctuations of eigenvalues on microscopic scale (i.e., on the scale of the average level spacing) are believed to display universal characteristics. It is our conjecture that the eigenvalues near zero virtuality respect such microscopic universality. This implies that the detailed dynamics of the QCD partition function are not important for the description of such fluctuations, and that they can be described equally well with a random matrix ensemble which respects the global symmetries of the QCD Dirac operator. In particular, the

following properties are included [8]: (i) the chiral structure of the Dirac operator leading to an eigenvalue spectrum $\pm\lambda_n$, (ii) the zero-mode structure of the Dirac operator (in the sector of topological charge ν the Dirac operator has exactly ν zero eigenvalues all of the same chirality), (iii) the flavor chiral symmetry and its spontaneous or explicit breaking, (iv) the reality type of the representation of the gauge group. For $SU(N_c)$, $N_c \geq 3$ in the fundamental representation, the gauge field is complex and so are the matrix elements of the Dirac operator. The gauge group $SU(2)$ in the fundamental representation is pseudoreal leading to matrix elements of the Dirac operator that are real. Finally, for gauge group $SU(N_c)$ in the adjoint representation, the gauge field is real and the matrix elements of the Dirac operator can be organized into real quaternions.

In this work we wish to construct a model which describes the fluctuations of the smallest eigenvalues as a function of the temperature. Near T_c , the theory of critical phenomena tells us that the fluctuations are universal with

nontrivial critical exponents, which are related to the propagation of soft modes. However, the recent work of Kocic and Kogut [5] suggests that this scenario may not be valid for phase transitions involving bosons composed of fermions. Instead, the lowest Matsubara frequency, πT , cures the infrared divergences and leads to a mean-field-like second-order phase transition. According to their work on the three-dimensional Gross-Neveu model, the dynamics of the phase transition are determined by the lowest Matsubara frequency. In this spirit, the only temperature effect we include in our model is that of the lowest Matsubara frequencies, $\pm\pi T$, between each pair of suitably chosen basis states $(1 \pm \gamma_5)\phi_n$. In the sector of topological charge ν , our basis must be complemented by ν unpaired basis states of the same chirality. Together with the symmetries mentioned above, this leads to the random matrix model (note that the sign of the negative Matsubara frequency has been absorbed in W by a unitary transformation),

$$Z_\beta(\nu, N_f) = \int \mathcal{D}W \det^{N_f} \begin{pmatrix} \mathbf{m}^* & iW + i\pi T \\ iW^\dagger + i\pi T & \mathbf{m} \end{pmatrix} \exp\left(-\frac{n\beta\Sigma^2}{2} \text{Tr}WW^\dagger\right), \quad (2.3)$$

where W is an $n \times (n + \nu)$ matrix. The integration over W is to be performed according to the Haar measure. We also include an arbitrary complex mass matrix \mathbf{m} with mass eigenvalues equal to m_f . For QCD with $N_c = 2$ the matrix elements of W are real ($\beta = 1$). They are complex for $N_c \geq 3$ ($\beta = 2$). In each case we include fermions in the fundamental representation. In our model, the number of modes per unit volume, $(2n + \nu)/V$, is identically 1. (Here, the Euclidean space-time volume is denoted by V .) Therefore, the thermodynamic limit corresponds to $n \rightarrow \infty$ (the topological charge $\nu \ll n$). The correct dimensions of physical quantities are obtained by multiplication with appropriate powers of the density of modes.

The fermion determinant in (2.3) can be written as a Grassmann integral:

$$Z_\beta(\nu, N_f) = \int \mathcal{D}W \mathcal{D}\psi^* \mathcal{D}\psi \exp\left[i \sum_{k=1}^{N_f} \psi^{k*} \begin{pmatrix} -i\mathbf{m}^* & W + \pi T \\ W^\dagger + \pi T & -i\mathbf{m} \end{pmatrix} \psi^k\right] \exp\left(-\frac{n\beta\Sigma^2}{2} \text{Tr}WW^\dagger\right). \quad (2.4)$$

The quenched approximation is obtained from this model as in the replica trick. We calculate a property for arbitrary N_f and take the limit $N_f \rightarrow 0$ at the end of the calculation. In particular, quantities which are N_f -independent are valid for $N_f = 0$ as well.

It should be stressed that the partition function (2.3) represents a *schematic* model for the chiral phase transition. Although the temperature dependence of this model does not coincide with that of chiral perturbation theory [11], it will be shown below that there is considerable qualitative agreement.

III. ANALYTIC RESULTS

In this section we evaluate the partition function (2.4) using methods which are standard in the supersymmetric formulation of random matrix theory [12,13]. The first step is to perform the average over W by performing a Gaussian integral. This leads to a four-fermion interaction. After averaging over the matrix elements of the Dirac operator, the partition function becomes

$$Z_1(\nu, N_f) = \int \mathcal{D}\psi^* \mathcal{D}\psi \exp\left(-\frac{1}{2n\Sigma^2\beta} (\psi_{Ri}^{f*} \psi_{Lk}^f \psi_{Ri}^{g*} \psi_{Lk}^g + 2\psi_{Ri}^{f*} \psi_{Lk}^f \psi_{Lk}^{g*} \psi_{Ri}^g + \psi_{Lk}^{f*} \psi_{Ri}^f \psi_{Lk}^{g*} \psi_{Ri}^g) + \mathbf{m}_{fg}^* \psi_{Ri}^{f*} \psi_{Ri}^g + \mathbf{m}_{fg} \psi_{Lk}^{f*} \psi_{Lk}^g + i\pi T (\psi_{Ri}^{f*} \psi_{Li}^f + \psi_{Lk}^{f*} \psi_{Rk}^f)\right), \quad (3.1)$$

for $\beta = 1$, and

$$Z_2(\nu, N_f) = \int \mathcal{D}\psi^* \mathcal{D}\psi \exp\left(-\frac{2}{n\Sigma^2\beta} \psi_{Lk}^{f*} \psi_{Ri}^f \psi_{Ri}^{g*} \psi_{Lk}^g + \mathbf{m}_{fg}^* \psi_{Ri}^{f*} \psi_{Ri}^g + \mathbf{m}_{fg} \psi_{Lk}^{f*} \psi_{Lk}^g + i\pi T (\psi_{Ri}^{f*} \psi_{Li}^f + \psi_{Lk}^{f*} \psi_{Rk}^f)\right) \quad (3.2)$$

for $\beta = 2$. In both cases, each of the four-fermion terms can

be written as the difference of two squares. Each square can be linearized by the Hubbard-Stratonovitch transformation according to

$$\exp(-AQ^2) \sim \int d\sigma \exp\left(-\frac{\sigma^2}{4A} - iQ\sigma\right). \quad (3.3)$$

For $\beta=2$, the partition function, expressed in terms of the two bosonic variables, can be combined into a single, complex $N_f \times N_f$ matrix, A , resulting in

$$\begin{aligned} Z_2(\nu, N_f) = & \int \mathcal{D}A \mathcal{D}\psi \mathcal{D}\psi^* \exp\left(-\frac{n\Sigma^2\beta}{2} \text{Tr}AA^\dagger\right. \\ & + \psi_{Lk}^{f*} \psi_{Lk}^g(A + \mathbf{m}) + \psi_{Ri}^{f*} \psi_{Ri}^g(A^\dagger + \mathbf{m}^*) \\ & \left. + i\pi T(\psi_{Ri}^{f*} \psi_{Li}^f + \psi_{Lk}^{f*} \psi_{Rk}^f)\right). \end{aligned} \quad (3.4)$$

For $\beta=1$, six new bosonic matrix variables are required. This is related to the fact that, for two colors, baryons are composed of two quarks and are bosons. They can be combined into one antisymmetric, complex $2N_f \times 2N_f$ matrix A , resulting in the partition function

$$\begin{aligned} Z_1(\nu, N_f) = & \int \mathcal{D}A \mathcal{D}\psi \mathcal{D}\psi^* \exp\left(-\frac{n\Sigma^2\beta}{2} \text{Tr}AA^\dagger\right) \exp\left[\frac{1}{2} \begin{pmatrix} \psi_R \\ \psi_R^* \end{pmatrix} (A^\dagger + \mathcal{M}^*) \begin{pmatrix} \psi_R \\ \psi_R^* \end{pmatrix}\right] \\ & \times \exp\left[\frac{1}{2} \begin{pmatrix} \psi_L \\ \psi_L^* \end{pmatrix} \begin{pmatrix} 0 & -\mathbf{1} \\ \mathbf{1} & 0 \end{pmatrix} (-A + \mathcal{M}) \begin{pmatrix} 0 & \mathbf{1} \\ -\mathbf{1} & 0 \end{pmatrix} \begin{pmatrix} \psi_L \\ \psi_L^* \end{pmatrix}\right] \exp[i\pi T(\psi_{Ri}^{f*} \psi_{Li}^f + \psi_{Lk}^{f*} \psi_{Rk}^f)]. \end{aligned} \quad (3.5)$$

In this case the mass matrix is an antisymmetric matrix given by

$$\mathcal{M} = \begin{pmatrix} 0 & -\mathbf{m} \\ \mathbf{m} & 0 \end{pmatrix}. \quad (3.6)$$

Note also that the temperature-dependent term can be rewritten as

$$\frac{i\pi T}{2} \begin{pmatrix} \psi_L \\ \psi_L^* \end{pmatrix} \begin{pmatrix} 0 & -\mathbf{1} \\ \mathbf{1} & 0 \end{pmatrix} \begin{pmatrix} \psi_R \\ \psi_R^* \end{pmatrix} - (L \leftrightarrow R). \quad (3.7)$$

Using this, the fermionic integrals can be performed, and the partition function is given by

$$\begin{aligned} Z_2(\nu, N_f) = & \int \mathcal{D}A \exp\left(-\frac{n\Sigma^2\beta}{2} \text{Tr}AA^\dagger\right) \\ & \times \det^{|\nu|}(A + \mathbf{m}) \det^n \begin{pmatrix} A + \mathbf{m} & \pi iT \\ \pi iT & A^\dagger + \mathbf{m}^* \end{pmatrix} \end{aligned} \quad (3.8)$$

for $\beta=2$, and

$$\begin{aligned} Z_1(\nu, N_f) = & \int \mathcal{D}A \exp\left(-\frac{n\Sigma^2\beta}{2} \text{Tr}AA^\dagger\right) \\ & \times \text{Pf}^{|\nu|}(-A + \mathcal{M}) \text{Pf}^n \begin{pmatrix} A^\dagger + \mathcal{M}^* & \pi iT \\ -\pi iT & -A + \mathcal{M} \end{pmatrix} \end{aligned} \quad (3.9)$$

for $\beta=1$. In (3.8) A is an arbitrary complex matrix whereas in (3.9) A is an arbitrary antisymmetric complex matrix.

In each case the condensate is given by

$$\langle \bar{q}q \rangle = \frac{1}{2nN_f} \partial_m \ln Z, \quad (3.10)$$

where Z is evaluated for a diagonal mass matrix with equal diagonal matrix elements. In the limit $n \rightarrow \infty$, the condensate can be determined with the aid of a saddle-point approximation. The saddle-point equations for $\beta=2$ are given by

$$-\frac{n\beta\Sigma^2}{2} A + n(A + \mathbf{m})((A^\dagger + \mathbf{m})(A + \mathbf{m}) + \pi^2 T^2)^{-1} = 0. \quad (3.11)$$

An arbitrary complex matrix can be diagonalized by performing the decomposition

$$A = U\Lambda V^{-1}, \quad (3.12)$$

with all eigenvalues positive and U and V unitary matrices. We find that the solution of (3.11) yields $U=V=1$ with eigenvalues λ given by the positive roots of

$$\Sigma^2 \lambda [(\lambda + \mathbf{m})^2 + \pi^2 T^2] - \lambda - \mathbf{m} = 0. \quad (3.13)$$

In the chiral limit we find a critical point at

$$T_c = \frac{1}{\pi\Sigma}. \quad (3.14)$$

In order to calculate the condensate, we express the derivative of the partition function in (3.10) in terms of an average over A ,

$$\langle \bar{q}q \rangle = \frac{1}{2nN_f} \left\langle \text{Tr} \begin{pmatrix} A^\dagger & \pi iT \\ \pi iT & A \end{pmatrix}^{-1} \right\rangle. \quad (3.15)$$

Below T_c , the mass m can be neglected in the saddle-point equation, and we find

$$\langle \bar{q}q \rangle = \Sigma(1 - \pi^2 T^2 \Sigma^2)^{1/2}. \quad (3.16)$$

At T_c , the solution of the saddle-point equation develops a nonanalytic dependence on m resulting in the condensate

$$\langle \bar{q}q \rangle = \Sigma^{4/3} m^{1/3}. \quad (3.17)$$

Therefore, we reproduce the mean-field value for the critical exponent $\delta=3$.

For $\beta=1$ the saddle-point equation for the A integration is

$$-\frac{\beta \Sigma^2}{2} A + \frac{1}{2} (A + \mathcal{M})((A^\dagger + \mathcal{M})(A - \mathcal{M}) + \pi^2 T^2)^{-1} = 0. \quad (3.18)$$

This equation can be solved by diagonalizing the complex antisymmetric matrix A as $A = U\Lambda U$, where U is a unitary matrix. Here, Λ is an antisymmetric, standard matrix such that $\Lambda_{k,k+1} = -\Lambda_{k+1,k} = \lambda_k$ for $k=1, \dots, 2N_f-1$ with all other matrix elements equal to zero. A suitable redefinition of U can always be made such that all $\lambda_k \geq 0$. The condensate is calculated as in the case of $\beta=2$ with the same result both below and at T_c . Of course, it comes as no surprise that we obtain the mean field value for the critical exponent in this case as well.

IV. THE PHASE TRANSITION

In the remainder of this paper we describe the results of numerical investigations of the random matrix model (2.3). For $N_f \neq 0$, the determinantal weight must be included in the integration measure which is extremely costly. However, for $N_f=0$ the distribution functions are simple Gaussians, and only this case will be studied. We also restrict ourselves to the sector of zero total topological charge, $\nu=0$. Instead of a Gaussian distribution we use a rectangular distribution in our calculations. General universality arguments [14] imply that the shape of the distribution of the matrix elements does not affect the properties of our random matrix model, and we expect that the results for a rectangular distribution will be in complete agreement with those of the Gaussian distribution. Indeed, our calculations which were all performed using rectangular distributions with zero mean, reproduce the analytical results of the previous section.

We study in the quenched approximation the average spectral density, $\bar{\rho}(\lambda)$, of the operator

$$\begin{pmatrix} 0 & iW + i\pi T \\ iW^\dagger + i\pi T & 0 \end{pmatrix}, \quad (4.1)$$

where the W are complex matrix elements with real and imaginary parts distributed according to a rectangular distribution with zero mean and variance σ . All eigenvalues of the matrix (4.1) occur in pairs $\pm\lambda$ (or are zero when $\nu \neq 0$). At $T=0$ it can be shown, using arguments familiar from random matrix theory [17], that this density has a semicircular shape in the limit $n \rightarrow \infty$,

$$\bar{\rho}(\lambda) = \frac{1}{\pi\sigma^2} \sqrt{4n\sigma^2 - \lambda^2}, \quad (4.2)$$

where σ^2 is the variance of the matrix elements. In order to obtain a finite condensate, the spectral density near zero must be proportional to n for $n \rightarrow \infty$ [see Eq. (3.10)]. This can be achieved by scaling the matrix elements with $\sim 1/\sqrt{n}$. With this choice of scaling (i.e., $n\sigma^2 \rightarrow \text{const}$ for $n \rightarrow \infty$) the effect of the random matrix and the temperature on the spectrum of (4.1) is of the same order of magnitude, and the spectrum is stable in the limit $n \rightarrow \infty$. Among others, this follows from the n dependence of the numerical results to be discussed below. In particular, we choose both real and imaginary parts of the matrix elements to be distributed uniformly on the interval $[-1/2\sqrt{n}, 1/2\sqrt{n}]$. This results in the variance

$$\overline{|W_{ij}|^2} = \frac{1}{6n}, \quad (4.3)$$

where n is the dimension of the off-diagonal blocks. Comparing this to the variance of the Gaussian distribution (2.3), we can make the identification

$$\frac{1}{6n} = \frac{2}{n\beta\Sigma^2}, \quad (4.4)$$

which yields $\Sigma^2=6$ for $\beta=2$. According to (3.14) the critical temperature is thus $\pi T_c = 1/\sqrt{6} = 0.40824$.

In our numerical simulations, we choose $n=20$ for most calculations. In some cases, we have studied matrix ensembles up to $n=50$ in order to extrapolate to $n \rightarrow \infty$. The relatively small value of n allows us to study very large ensembles. In order to study the temperature dependence, the size of the ensemble for *each* temperature is 2×10^4 , whereas for some specific temperatures we take the size of the ensemble equal to 10^5 matrices. The diagonalization is carried out by standard methods [15].

Like in QCD, the chiral order parameter of our schematic model is the spectral density $\rho(0)$. It is related to the chiral condensate *via* the Banks-Casher formula [16]

$$\langle \bar{q}q \rangle = \lim_{\epsilon \rightarrow 0} \lim_{n \rightarrow \infty} \frac{1}{2n} \pi \rho(\epsilon), \quad (4.5)$$

where the order of the limits cannot be interchanged (see below). Let us first consider the complete spectral density, $\rho(\lambda)$. In Figs. 1(a)–1(c), we show numerical results for the complete spectral density for $\pi T=0$, $\pi T=0.4$, and $\pi T=1.0$. The full line in Fig. 1(a) shows the analytical result (4.2). For a nonzero temperature, it is somewhat more difficult to obtain the level density analytically¹ [19]. When T is large, we find that the distribution splits into two semicircles with centers at $+\pi T$ and $-\pi T$.

The deviations from a semicircle at $T=0$ are not statistical fluctuations but rather well-understood finite- n corrections [18]. (The statistical errors are about 0.5%.) These deviations

¹The analytical result for $\rho(\lambda)$ at finite n is a four-dimensional integral [19]. For $n \rightarrow \infty$ these integrals can be performed by a saddle-point approximation. The result is given by $\rho(\lambda) = -(2n/\pi) \text{Im} G(\lambda + i0)$ where the resolvent $G(z) \equiv (1/2n) \text{Tr}[1/(z-H)]$ [with H the matrix in (4.1)] satisfies the third-order polynomial equation $n^2 \sigma^4 G^3(z) - 2n \sigma^2 z G^2(z) + G(z)(n \sigma^2 - \pi^2 T^2 + z^2) - z = 0$.

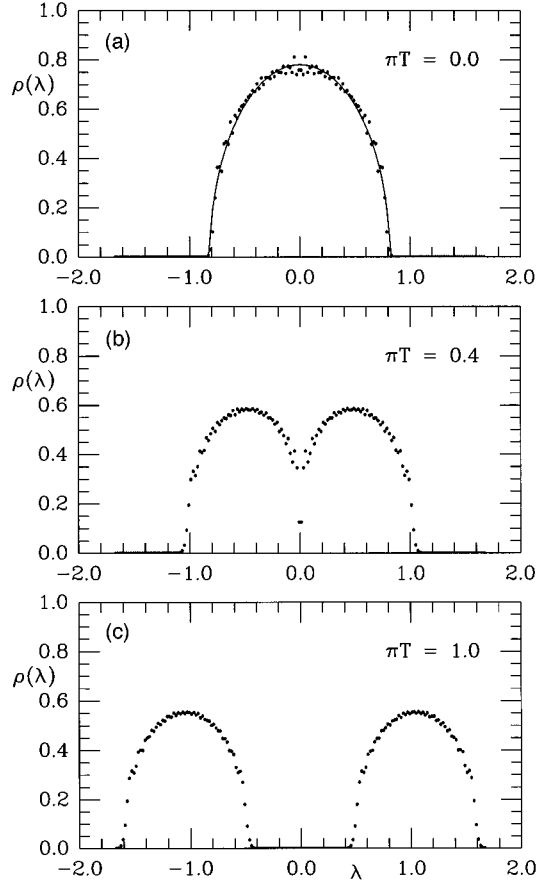


FIG. 1. Histograms of the complete spectrum of eigenvalues obtained for $n=20$ at temperatures of (a) $\pi T=0$ (top curve), (b) $\pi T=0.4$ (middle curve), and (c) $\pi T=1.0$ (bottom curve). Each spectrum was obtained from 10^5 matrices.

occur on the the scale of the spacing between two neighboring eigenvalues and can be expressed analytically in terms of Bessel functions which show oscillations on this scale. At the moment, we wish to remark only that the behavior near zero is given by $\bar{\rho}(\lambda) \sim N\lambda$ which emphasizes the importance of the order of the limits in the Banks-Casher formula. In practice we have obtained $\rho(0)$ from the first few bins beyond the bin containing the average position of the first eigenvalue using a histogram bin size equal to 0.02.

According to the mean-field argument presented in Sec. III, our model shows a second-order phase transition with

$$\rho(0, T) \sim \sqrt{T_c^2 - T^2}. \quad (4.6)$$

In order to account for finite- n effects approximately, we convolute this expression with a Gaussian

$$\rho_\sigma(0, T) \sim \int_{-T_c}^{T_c} dx \sqrt{T_c^2 - x^2} \exp[-(x-T)^2/\sigma^2]. \quad (4.7)$$

While we offer no analytic justification for this form, we note that it provides an excellent fit to the results of simulations. The χ^2 per data point is equal to 1.65. The statistical error in $\langle \bar{q}q \rangle$ follows from the error in the spectral density and is about 1%. A best fit of (4.7) to our results for $n=20$ is shown in Fig. 2. In this case, the fitted values for πT_c and σ

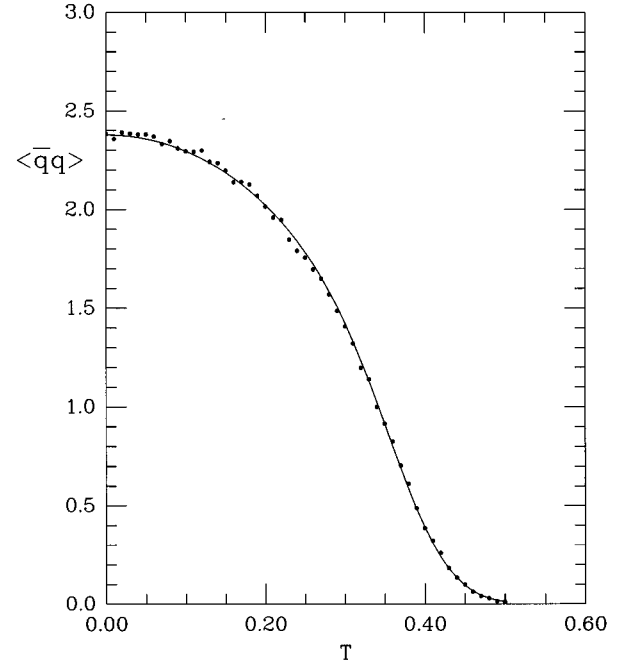


FIG. 2. The $\langle \bar{q}q \rangle$ condensate as calculated from (4.3) for $n=20$. Each point was obtained on the basis of 2×10^4 matrices, and $\rho(0)$ was obtained by counting eigenvalues in the range $0 \leq \lambda \leq 0.02$. The solid curve is a fit according to (4.7) using the parameters $T_c=0.3890$ and $\sigma=0.7414$.

are 0.389 and 0.074, respectively. Using data for $n \leq 50$ we performed an extrapolation to $n \rightarrow \infty$ according to the expression

$$T_c^n = T_c^\infty \left(1 + \frac{\alpha}{n} \right), \quad (4.8)$$

where α is a constant to be determined. We find a critical temperature of $\pi T_c^\infty = 0.3976$ which is in good agreement with the theoretical value of $\pi T_c = 1/\sqrt{6} = 0.4083$ for our present numerical parameters.

Recent lattice QCD calculations [2] have studied the condensate as a function of the so-called valence mass. In these lattice simulations, the sea-quark mass was much larger than the smallest eigenvalue so that the problem is effectively equivalent to taking $N_f=0$. It is possible to simulate these calculations within the framework of the present model by defining

$$\langle \bar{\psi}\psi \rangle_m = \frac{1}{n} \sum_{k=1}^n \frac{m}{\lambda_k^2 + m^2}. \quad (4.9)$$

If we take the limits $\lim_{m \rightarrow 0} \lim_{n \rightarrow \infty}$ in this order, we reproduce the Banks-Casher formula [16]. For finite n and masses below the smallest eigenvalue (see next section for its distribution) $\langle \bar{\psi}\psi \rangle_m \sim m$. This is indeed what is seen in Fig. 3 where we show a log-log plot of the resulting values for $\langle \bar{\psi}\psi \rangle$ as a function of m for $n=20$. Our results are qualitatively similar to the lattice calculations. At finite n the $m \rightarrow 0$ limit has to be taken with care in the sense that masses below the smallest eigenvalue cannot be used in the extrapolation

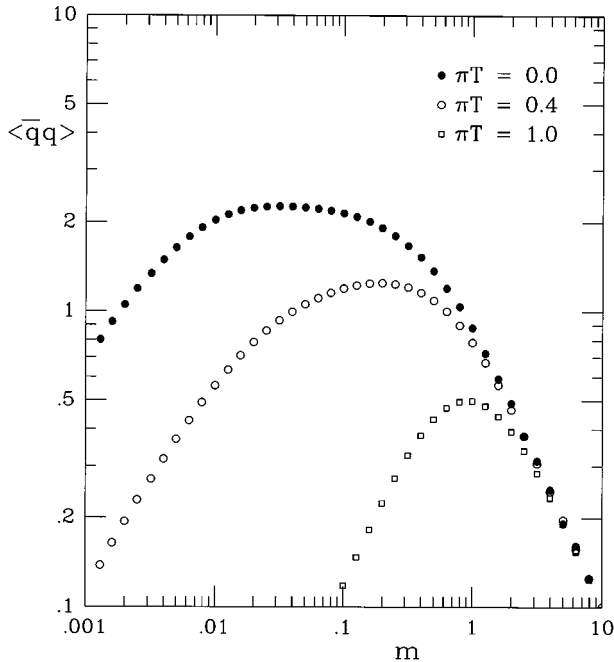


FIG. 3. The condensate as a function of the so-called valence quark mass calculated according to (4.9) at $\pi T=0$, $\pi T=0.4$, and $\pi T=1.0$. The calculations were performed for $n=20$ and 2×10^4 matrices were used for each temperature.

the $m \rightarrow 0$. These results show that the spectral density yields a much more accurate determination of the chiral condensate [20].

V. DYNAMICS OF THE SMALLEST EIGENVALUE

In this section we study the distribution of the eigenvalue of smallest magnitude, denoted by λ_1 , as a function of temperature. This distribution is known analytically for a few special cases of the Laguerre ensemble. The present case, defined by the random matrix model (2.3) for $N_f=0$, at $T=0$ happens to be one of them. With our choice of parameters, the distribution is given by [21]

$$f(\lambda_1) \sim \lambda_1 \exp\left(-\left(\frac{n\beta\Sigma\lambda_1}{2}\right)^2\right). \quad (5.1)$$

This $T=0$ result is exact even for finite n . (The factor of λ_1 is readily understood. For every eigenvalue $+\lambda$ there is always a corresponding eigenvalue of $-\lambda$. This factor is simply a consequence of level repulsion.) In order to be able to describe the temperature dependence, we introduce a more general distribution

$$f(\lambda_1) = \lambda_1 \exp\left(-\frac{(\lambda_1 - x_0)^2}{\sigma^2}\right). \quad (5.2)$$

At zero temperature $x_0=0$ and $\sigma=2/n\beta\Sigma$. The average value of the smallest eigenvalue is given as $\lambda_1 = \sqrt{\pi/n\beta\Sigma}$. While this expression is not, in general, exact, it is serviceable.

In Fig. 4 we show a histogram of the distribution of the smallest eigenvalue at $T=0$ for the case $n=20$. The results are in excellent agreement with (5.1). The temperature de-

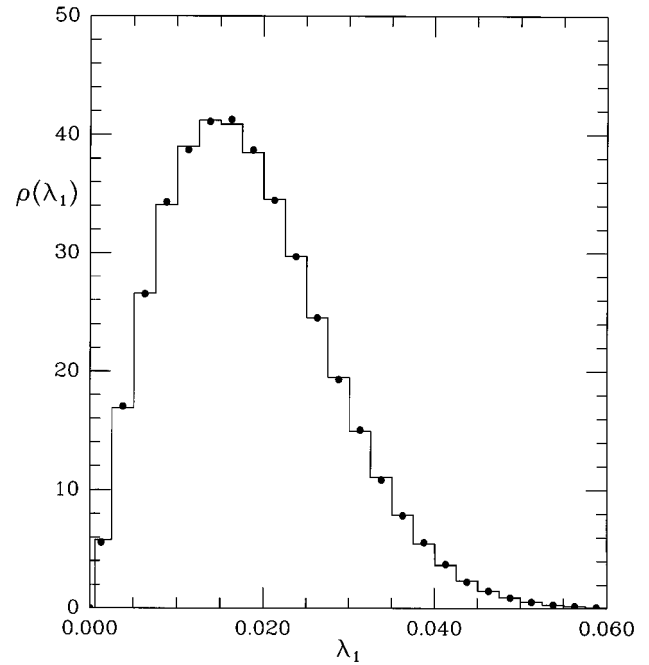


FIG. 4. The distribution of the eigenvalue of smallest magnitude determined from 2×10^5 trials with $n=20$ for a bin size of 0.02 (points). The histogram was obtained from (5.2) with $x_0=0$. The value of $\sigma=0.020685$ was determined from the average value of λ_1 obtained from the simulations. This fitted value is in excellent agreement with the analytic value of $2/n\beta\Sigma=0.02041\dots$. The form of (5.2) provides an excellent fit to the simulation data with $\chi^2=0.8$.

pendence of the parameters of the distribution is shown in Fig. 5, where we show the ratio $\lambda_1/\Delta\lambda_1$ as a function of the temperature for $n=10$. When $x_0=0$ this ratio is equal to $[\pi/(4-\pi)]^{1/2}=1.913\dots$. Surprisingly, we find that this ratio is constant for $T < T_c$. This implies that x_0 is strictly zero for $T < T_c$. Inspection of the corresponding distribution indicates that (5.1) remains quantitatively valid in this region. Above this temperature (and ignoring some finite n effects near threshold), x_0 grows linearly with T . This behavior is expected since the entire distribution moves linearly with T for sufficiently large T . What is surprising is that x_0 vanishes below some finite T , and that the effect is so pronounced for a matrix of such small dimension.

The behavior of $x_0(T)$ versus T (shown in Fig. 6) allows us to extract T_c from $x(T_c)=0$. In practice we use a linear extrapolation of our data for $T > T_c$. Our results for different size matrices can be summarized by the expression

$$\pi T_c^{(n)} = 0.40859 \frac{n + 2.51316}{n + 4.10346}, \quad (5.3)$$

which yields an asymptotic result of $\pi T_c=0.40859$, which is very close to the theoretical result of $1/\sqrt{6}=0.40824$. [The constants in (5.3) have been obtained by minimizing the χ^2 of this expression using the results obtained for T_c^n for $n=10, 20, 30, 40$, and 50 .]

As indicated, the form of (5.2) is not exact. Similar results can be obtained in a model-independent fashion by straight-

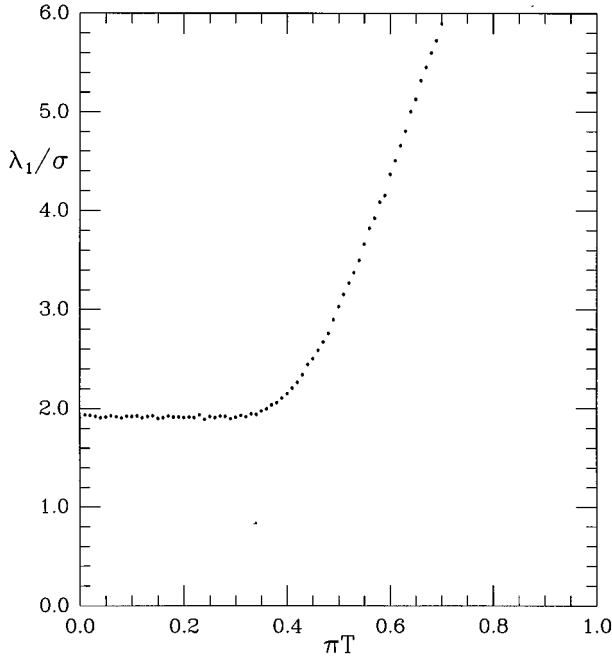


FIG. 5. The ratio of the smallest eigenvalue to its rms deviation, $\overline{\lambda_1}/\Delta\lambda_1$, as a function of temperature for $n=10$. Each point represents 2×10^4 matrices. The average value of this ratio for $T < T_c$ is 1.9107 which is in good agreement with the expected value of $\sqrt{\pi/(4-\pi)} = 1.913 \dots$

line extrapolation of the observed values of $\overline{\lambda_1}/\Delta\lambda_1$ as a function of the temperature.

Finally, we study the scaling of the smallest eigenvalue with n . For temperatures of $0.9T_c$, T_c , and $1.1T_c$ we study ensembles of each 2×10^4 matrices with dimensions $n=10, 12, 15, 19, 24, 30, 37, 45$, and 54 .

For $T < T_c$, the Banks-Casher formula suggests that $\lambda_{\min} \sim 1/n$ leading to the same n dependence for the expectation value and the variance of λ_{\min} . Numerically, the exponent of the leading n dependence of the mean and the variance for is obtained by fitting the expression

$$\frac{\alpha}{n^\gamma} + \frac{\beta}{n^{\gamma+1}} \quad (5.4)$$

to the data for $T=0.9T_c$. For the mean we find $\gamma=1.013 \pm 0.020$ ($\alpha=2.058$ and $\beta=-3.429$), and for the variance $\gamma=1.012 \pm 0.020$ ($\alpha=1.228$ and $\beta=-2.390$). Both results are in agreement with the theoretical value of $\gamma=1$.

At $T=T_c$ we have $\Sigma(m) \sim m^{1/\delta}$. This leads to the eigenvalue density (for $\lambda \rightarrow 0$)

$$\rho(\lambda) \sim m^{\alpha_1} \lambda^{\alpha_2} \quad \text{with} \quad \alpha_1 + \alpha_2 = \frac{1}{\delta}. \quad (5.5)$$

Smaller masses suppress the eigenvalue density near zero, so we must have $\alpha_1 > 0$. For a fixed mass, the eigenvalue density should not diverge, so we must also have $\alpha_2 > 0$. It is possible that α_1 and α_2 depend on N_f , but we were not able to investigate this point within the present framework. The scaling behavior of the smallest eigenvalue is obtained from $\int_0^{\lambda_{\min}} \rho(\lambda) d\lambda \sim 1/n$ which leads to

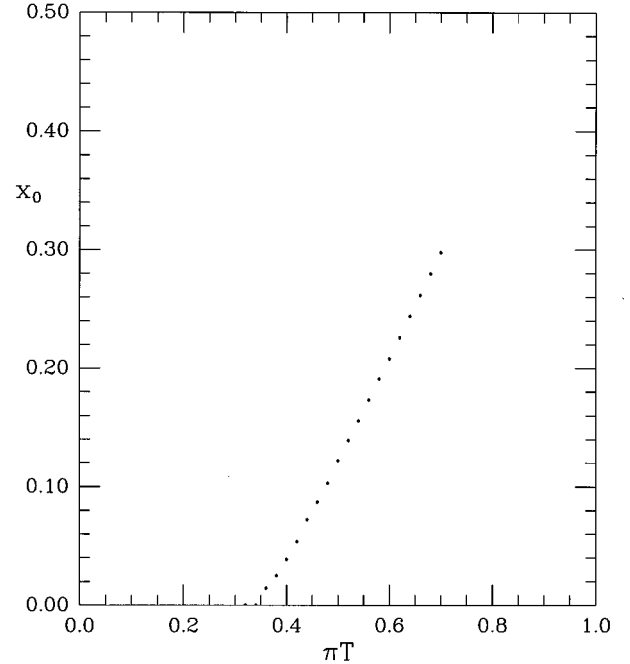


FIG. 6. The parameter x_0 of (5.2) as a function of T for $n=10$. Each point represents 2×10^4 matrices. The parameters x_0 and σ were determined from the ratio $\overline{\lambda_1}/\Delta\lambda_1$ (shown in Fig. 5) and the corresponding values of $\overline{\lambda_1}$. Linear extrapolation suggests $\pi T_c = 0.3625$ for this case.

$$\langle \lambda_{\min} \rangle \sim n^{-1/(\alpha_2+1)}. \quad (5.6)$$

For $N_f=0$, the eigenvalue density cannot depend on m and we thus have $\alpha_2=1/\delta$ and $\alpha_1=0$ for $N_f=0$. This yields

$$\langle \lambda_{\min} \rangle \sim n^{-\delta/(1+\delta)}. \quad (5.7)$$

From the analytical result for δ [see (3.17)] we find $\langle \lambda_{\min} \rangle \sim n^{-3/4}$. Numerically, δ is obtained by fitting our results for different values of n by the expression α/n^γ . By minimizing the χ^2 we find $\gamma=0.753 \pm 0.004$ ($\alpha=1.228$), leading to $\delta=3.05 \pm 0.07$, in perfect agreement with the theoretical result. The ratio of the mean and the variance of the smallest eigenvalue at this temperature is constant within 0.5% resulting in the same value of γ for the variance ($\alpha=0.558$ in this case).

For $T > T_c$ the average position of the smallest eigenvalue departs from zero and scales like n^0 . We expect [22] that its variance will have the scaling behavior $n^{-2/3}$ which is typical for eigenvalues near the edge of a semicircle. Indeed, fitting our numerical results for the variance of the smallest eigenvalue for $T=1.1T_c$ with α/n^γ yields $\gamma=0.677 \pm 0.003$ ($\alpha=0.519$), in perfect agreement with the theoretical expectation. The average position of the smallest eigenvalue has been fitted by $\alpha + \beta/n^\gamma$. We find $\alpha=0.0356 \pm 0.0016$ and $\gamma=0.723 \pm 0.009$ ($\beta=1.246$).

VI. CONCLUSIONS

In this paper, we have studied a random matrix model which possesses the global symmetries of the QCD action and the temperature dependence suggested by the form of the lowest Matsubara frequency. At $T=0$ this model is com-

pletely soluble; it reduces to what is known in the mathematical literature as the Laguerre ensemble. For nonzero temperatures, we have succeeded in extracting some interesting properties analytically. In particular, we have shown that the model undergoes a second-order phase transition with mean-field critical exponents $\beta=1/2$ and $\delta=3$. The lattice result [1] for QCD with two light flavors for $1/\beta\delta$ is 0.77 ± 0.14 , which is closer to these mean-field values than to the results for either the O(4) or O(2) Heisenberg spin models. For three or more light flavors, QCD shows a first-order chiral phase transition, whereas for one flavor there is no transition at all. Our model does not contain such flavor dependence: It has a second-order phase transition for any number of flavors. If our model has anything to say about QCD, it is for QCD with two light flavors.

Numerically, we found one surprising result: The distribution of the smallest eigenvalue below T_c is (numerically)

equivalent to the distribution obtained for $T=0$. For $T>T_c$, the centroid of its Gaussian distribution grows linearly with T . The behavior at $T=0$ agrees well with known analytical results.

Our results suggest an alternative method for obtaining the critical temperature; namely, from the distribution of the eigenvalue of smallest magnitude. It would be interesting to study the dynamics of the smallest eigenvalues in lattice QCD as well.

ACKNOWLEDGMENTS

The reported work was partially supported by the US DOE Grant No. DE-FG-88ER40388. We would like to thank H. A. Weidenmüller and T. Wettig for useful discussions and for communicating their results on a related model prior to publication.

-
- [1] F. Karsch and E. Laermann, *Phys. Rev. D* **50**, 6954 (1994).
 - [2] S. Chandrasekharan, in *Continuous Advances in QCD*, edited by A. Smilga, (World Scientific, Singapore, 1994).
 - [3] R. D. Pisarski and F. Wilczek, *Phys. Rev. D* **29**, 338 (1984).
 - [4] K. Rajagopal and F. Wilczek, *Nucl. Phys. B* **399**, 395 (1993).
 - [5] A. Kocic and J. Kogut, *Phys. Rev. Lett.* **74**, 3109 (1995), *Nucl. Phys. B* **455**, 229 (1995).
 - [6] S. J. Hands and M. Teper, *Nucl. Phys.* **B347**, 819 (1990).
 - [7] T. Kalkreuter, *Phys. Rev. D* **51**, 1305 (1995); *Phys. Lett. B* **276**, 485 (1992); *Phys. Rev. D* **48**, 1926 (1993).
 - [8] J. Verbaarschot, *Phys. Rev. Lett.* **72**, 2531 (1994); *Phys. Lett. B* **329**, 351 (1994); *Nucl. Phys.* **B426**, 559 (1994); **B427**, 434 (1994).
 - [9] A. Halasz and J. J. M. Verbaarschot, *Phys. Rev. D* **52**, 2563 (1995).
 - [10] H. Leutwyler and A. Smilga, *Phys. Rev. D* **46**, 5607 (1992).
 - [11] J. Gasser and H. Leutwyler, *Phys. Lett. B* **188**, 477 (1987).
 - [12] K. B. Efetov, *Adv. Mod. Phys.* **32**, 53 (1983).
 - [13] J. Verbaarschot, H. Weidenmüller, and M. Zirnbauer, *Phys. Rep.* **129**, 367 (1985).
 - [14] E. Brézin and A. Zee, *Nucl. Phys.* **B402**, 613 (1993); C. Beenhakker, *ibid.* **B422**, 515 (1994); G. Hackenbroich and H. Weidenmüller, *Phys. Rev. Lett.* **74**, 4118 (1995).
 - [15] B. T. Smith, J. M. Boyle, J. J. Dongarra, B. S. Garbow, Y. Ikebe, V. C. Klema, and C. B. Moler, *Matrix Eigensystems Routines—EISPACK Guide* (Springer-Verlag, New York, 1976).
 - [16] T. Banks and A. Casher, *Nucl. Phys.* **B169**, 103 (1980).
 - [17] M. Mehta, *Random Matrices* (Academic Press, San Diego, 1991).
 - [18] J. J. M. Verbaarschot and I. Zahed, *Phys. Rev. Lett.* **70**, 3852 (1993).
 - [19] A. D. Jackson, M. Sener, and J. J. M. Verbaarschot, *Phys. Lett. B* **368**, 137 (1996).
 - [20] J. J. M. Verbaarschot, “Universality near zero virtuality,” Institution Report No. SUNY-NTG-96/1 (unpublished).
 - [21] P. J. Forrester, *Nucl. Phys.* **B402**, 709 (1993).
 - [22] J. J. M. Verbaarschot and M. R. Zirnbauer, *Ann. Phys.* **158**, 78 (1984).